

# Anti-Holomorphic Modes in Vortex Lattices

Brook J. Hocking<sup>1</sup> and Thomas Machon<sup>1,\*</sup>

<sup>1</sup>*H.H. Wills Physics Laboratory, University of Bristol, Tyndall Avenue, Bristol BS8 1TL, UK*

A continuum theory of linearized Helmholtz-Kirchoff point vortex dynamics about a steadily rotating lattice state is developed by two separate methods: firstly by a direct procedure, secondly by taking the long-wavelength limit of Tkachenko's exact solution for a triangular vortex lattice. Solutions to the continuum theory are found, described by arbitrary anti-holomorphic functions, and give power-law localized edge modes. Numerical results for finite lattices show excellent agreement to the theory.

## INTRODUCTION

Helmholtz-Kirchoff dynamics of point vortices [1] in a two-dimensional ideal fluid serve as a model for vortex dynamics in superfluid helium [2], Bose-Einstein condensates [3] and magnetized non-neutral plasmas [4, 5], are related to turbulence [6] and are also of independent mathematical interest [7, 8]. In an unbounded domain, there can be no finite stationary collection of vortices, instead vortex crystals [9] are found, patterns of vortices undergoing steady rigid-body motion. For large numbers of vortices, stable vortex crystals assume the form of distorted triangular lattices [10–12], and in the infinite limit a perfect triangular lattice is an exact, stable solution, as shown by Tkachenko [13, 14].

Tkachenko studied the behaviour of  $\ell^2$  perturbations of the infinite vortex lattice, amenable to Fourier analysis, with the result that any such perturbation may be decomposed into Tkachenko waves [14–18], plane waves where the vortices trace out elliptic paths, suggested to be related to oscillations in pulsars [19–21]. Here, the linearized dynamics of a large, but finite, lattice in an unbounded domain is studied. We show that in such a system a set of additional modes appears, described by arbitrary anti-holomorphic functions, and corresponding to power-law confined edge modes. In the continuum limit for very large (but still finite) lattices this correspondence is exact, and arbitrary anti-holomorphic functions form a degenerate eigenspace. In the laboratory frame these modes are zero-frequency, coupled with the overall rotation of the lattice leads to a time dependent deformation structure rotating in the same direction as the lattice, but at a slower frequency.

Liouville's theorem ensures that the anti-holomorphic modes do not exist in an infinite system, the magnitude of any non-constant anti-holomorphic mode is unbounded, so cannot arise as a lattice perturbation. However, their existence is revealed in the bulk spectrum, a kind of bulk-boundary correspondence. Special points in the Brillouin zone where the Hamiltonian operator  $H(k)$  is defective (non-diagonalizable) have been related to edge modes [22–24]. In the vortex lattice there is a defective singularity at

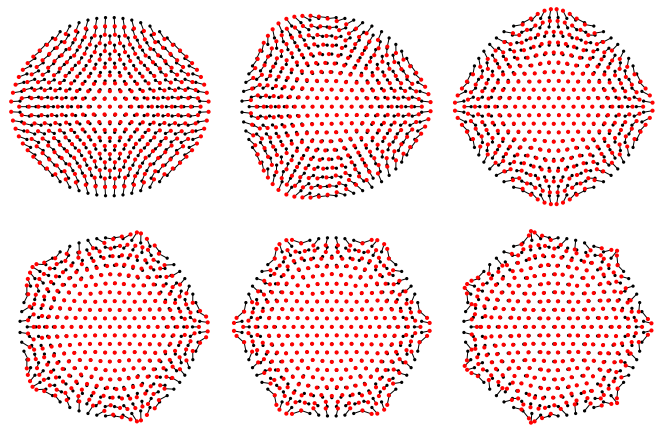


Figure 1. Anti-holomorphic modes  $\bar{z}^n$ ,  $1 \leq n \leq 6$ , found numerically for a steadily rotating vortex crystal,  $N = 331$ . Equilibrium vortex positions given by black points, displacement under the anti-holomorphic mode given by red points.

$k = 0$ . The limit

$$\lim_{|k| \rightarrow 0} H(k), \quad (1)$$

is not unique, it yields a defective Hamiltonian, the form of which depends on the direction of approach to 0. This singularity can be attributed to the long-range nature of the vortex interactions, and the local behaviour around  $k = 0$  leads to the anti-holomorphic modes.

We study these modes by developing a continuum theory via two separate methods, firstly by a direct approach and secondly by coarse-graining Tkachenko's exact solution [13, 14]. We note that the theory is a linearization of the point-vortex dynamics, rather than a hydrodynamical theory [25–28].

Numerics confirm the existence of anti-holomorphic modes (Figs. 1, 2, and 3), and show excellent agreement to the theory as well as earlier numerical results [29, 30]. Microscopic details of finite lattices lead to a splitting of the degenerate space of anti-holomorphic modes, consequently eigenmodes of the finite lattice appear as power-law confined edge modes. There are other descriptions

of chiral edge waves in vortex matter which do not connect them to anti-holomorphic modes; Campbell developing a continuum theory with Krasnov [17, 31, 32], with related work by Casalilla on surface modes of vortex matter [33]. Continuum theories [25, 26] of vortex matter have found edge modes described by the Benjamin-Davis-Ono equation [34], and there has been work on statistical edge modes [35], exploiting the anomalous statistical mechanics of vortices [36]. The modes we describe are reminiscent of conformal crystals, numerically observed in vortex lattices in superconductors [37]. In compressible systems the dynamics changes [38–41], however the modes we observe are likely related to the gapped Kohn modes found in compressible vortex lattices [17, 42].

## CONTINUUM THEORY OF LATTICE MODES

We begin with the motion of a finite collection of vortices in the plane. Let  $p_\alpha = x_\alpha + iy_\alpha \in \mathbb{C}$  be the position of vortex  $\alpha$ , its motion is then given by

$$\dot{\bar{p}}_\alpha = \frac{1}{2\pi i} \sum_{\beta \neq \alpha} \frac{\Gamma_\beta}{p_\alpha - p_\beta}, \quad (2)$$

where  $\Gamma_\beta$  is the strength of vortex  $\beta$  and  $\bar{p}$  is the complex conjugate of  $p$ . This can be written as a Hamiltonian system

$$\Gamma_\alpha \frac{dx_\alpha}{dt} = \frac{\partial H}{\partial y_\alpha}, \quad \Gamma_\alpha \frac{dy_\alpha}{dt} = -\frac{\partial H}{\partial x_\alpha}, \quad (3)$$

with Hamiltonian

$$H = -\frac{1}{4\pi} \sum_{\alpha, \beta, \alpha \neq \beta} \Gamma_\alpha \Gamma_\beta \log |p_\alpha - p_\beta|. \quad (4)$$

(In the sum each pair  $(\alpha, \beta)$  is counted twice, hence  $1/4\pi$ , not  $1/2\pi$ .) Anticipating a steadily rotating vortex crystal with angular velocity  $\Omega$ , we write

$$p_\alpha(t) = e^{i\Omega t} z_\alpha(t). \quad (5)$$

This gives the equations of motion in the rotating frame

$$\dot{\bar{z}}_\alpha(t) = i\Omega \bar{z}_\alpha(t) + \frac{1}{2\pi i} \sum_{\beta \neq \alpha} \frac{\Gamma_\beta}{z_\alpha - z_\beta} \quad (6)$$

This is once again Hamiltonian, with

$$H_\Omega = \frac{\Omega}{2} \sum_\alpha \Gamma_\alpha |z_\alpha|^2 - \frac{1}{4\pi} \sum_{\alpha, \beta, \alpha \neq \beta} \Gamma_\alpha \Gamma_\beta \log |z_\alpha - z_\beta|. \quad (7)$$

A local minimum of  $H_\Omega$  describes a stable vortex crystal steadily rotating about the origin with angular velocity  $\Omega$ .

We suppose  $\{z_\alpha^0\}$  is such a local minimum, then expanding  $z_\alpha = z_\alpha^0 + \psi_\alpha$  to linear order in  $\{\psi_\alpha\}$  yields

$$\dot{\bar{\psi}}_\alpha(t) = i\Omega \bar{\psi}_\alpha(t) - \frac{1}{2\pi i} \sum_{\beta \neq \alpha} \frac{\Gamma_\beta}{(z_\alpha^0 - z_\beta^0)^2} (\psi_\alpha - \psi_\beta). \quad (8)$$

The equations for coarse-grained vortex dynamics are now derived. Two derivations are given. The first is a heuristic physical argument. The second is a derivation based on an explicit coarse-graining of Tkachenko's exact solution for the infinite lattice. Henceforth assume all vortices have identical vorticity  $\Gamma_\alpha = 2\pi$ , rescaling the vorticity is equivalent to changing the timescale.

### Derivation 1: Direct coarse-graining

We define the field

$$\chi(z, t) = \sum_\alpha \delta(z - z_\alpha^0) \psi_\alpha \quad (9)$$

where  $\delta(z - z_\alpha^0)$  is a Dirac-delta function at  $z_\alpha^0$ . The dynamics of  $\chi$  are given by

$$\dot{\bar{\chi}}(z, t) = i\Omega \bar{\chi}(z, t) + i \sum_{\alpha, \beta, \alpha \neq \beta} \frac{\delta(z - z_\alpha^0) (\psi_\alpha - \psi_\beta)}{(z_\alpha^0 - z_\beta^0)^2}. \quad (10)$$

We regularize with some small  $0 < \sigma \ll 1$ , with the idea that we take the limit  $\sigma \rightarrow 0$  and write

$$\dot{\bar{\chi}}(z, t) \approx i\Omega \bar{\chi}(z, t) + i \sum_{\alpha, \beta} \frac{\delta(z - z_\alpha^0) (\psi_\alpha - \psi_\beta)}{\sigma + (z_\alpha^0 - z_\beta^0)^2} \quad (11)$$

Defining  $\Delta(z) = \sum_\alpha \delta(z - z_\alpha^0)$ , we can then find

$$\dot{\bar{\chi}}(z, t) \approx i\Omega \bar{\chi}(z, t) + i \int_{\mathbb{C}} \frac{\chi(z, t) \Delta(w) - \Delta(z) \chi(w, t)}{\sigma + (z - w)^2} dA_w, \quad (12)$$

where  $z$  in the above equation is, for now, evaluated only at the points  $z_\alpha^0$ . We now consider the coarse-grained field

$$\Psi(z, t) = \frac{1}{A} \int_{D_z} \chi(w, t) dA, \quad (13)$$

where  $D_z$  is a disk of radius  $R$ , area  $A$ , centered at  $z$ .  $R$  is an appropriate lengthscale, to be determined. We then find the equations of motion

$$\dot{\bar{\Psi}}(z, t) = -i\Omega \bar{\Psi}(z, t) - i \frac{1}{A} \int_{D_z} \left( \int_{\mathbb{C}} \frac{\bar{\chi}(w) \Delta(v) - \Delta(w) \bar{\chi}(v)}{\sigma + (\bar{w} - \bar{v})^2} dA_v \right) dA_w. \quad (14)$$

By the definition of  $\chi$ , there exists a non-zero  $\delta$  on the lengthscale of the lattice spacing such that the numerator  $\bar{\chi}(w) \Delta(v) - \Delta(w) \bar{\chi}(v) = 0$  for  $|(w - z)| < \delta$ . We can then

safely take the limit  $\sigma \rightarrow 0$ . We also separate the inner integral into two pieces,

$$\begin{aligned} \dot{\Psi}(z, t) = & -i\Omega\Psi(z, t) \\ & -i\frac{1}{A}\int_{D_z}\left(\int_{D_w}\frac{\bar{\chi}(w)\Delta(v)-\Delta(w)\bar{\chi}(v)}{(\bar{w}-\bar{v})^2}dA_v\right)dA_w \\ & -i\frac{1}{A}\int_{D_z}\left(\int_{C\setminus D_w}\frac{\bar{\chi}(w)\Delta(v)-\Delta(w)\bar{\chi}(v)}{(\bar{w}-\bar{v})^2}dA_v\right)dA_w. \end{aligned} \quad (15)$$

We now coarse-grain, assuming that  $\chi(z)$  is a smooth function of  $z$  varying slowly on lengthscales of order  $R$ . Given the lattice cell area  $A_{\text{cell}}$ , define the density  $\rho = 1/A_{\text{cell}}$ . In the coarse-grained regime we then have

$$\begin{aligned} \dot{\Psi}(z, t) = & -i\Omega\Psi(z, t) \\ & -i\frac{\rho}{A}\int_{D_z}\left(\int_{D_w}\frac{\bar{\chi}(w)-\bar{\chi}(v)}{(\bar{w}-\bar{v})^2}dA_v\right)dA_w \\ & -i\frac{\rho}{A}\int_{D_z}\left(\int_{C\setminus D_w}\frac{\bar{\chi}(w)-\bar{\chi}(v)}{(\bar{w}-\bar{v})^2}dA_v\right)dA_w. \end{aligned} \quad (16)$$

Consider the second term. We can Taylor expand  $\chi$  as

$$\bar{\chi}(v) = \bar{\chi}(w) + \sum_{a,b \geq 0} c_{ab}(v-w)^a(\bar{v}-\bar{w})^b. \quad (17)$$

We can then perform the inner integral in the second term, to leading order only the  $c_{02}$  term contributes and we find

$$\begin{aligned} \dot{\Psi}(z, t) = & -i\Omega\Psi(z, t) - i\frac{A\rho}{2}\partial_{\bar{z}}^2\bar{\Psi}(z, t) \\ & -i\frac{\rho}{A}\int_{D_z}\left(\int_{C\setminus D_w}\frac{\bar{\chi}(w)-\bar{\chi}(v)}{(\bar{w}-\bar{v})^2}dA_v\right)dA_w. \end{aligned} \quad (18)$$

We now deal with the final term. Since  $\chi$  is approximately constant on lengthscales of  $R$ , we can approximate finding

$$\partial_t\Psi = -i\Omega\Psi - i\frac{\rho A}{2}\partial_{\bar{z}}^2\bar{\Psi} - i\rho\int_C\frac{\bar{\Psi}(z)-\bar{\Psi}(w)}{(\bar{z}-\bar{w})^2}dA_w. \quad (19)$$

By choosing  $A = 1/(4\pi\Omega)$  and rescaling time we can find

$$i\partial_t\bar{\Psi} = -\Omega\bar{\Psi} - 4\pi\Omega\int_C\frac{\bar{\Psi}(z)-\bar{\Psi}(w)}{(z-w)^2}dA_w - \frac{1}{2}\partial_z^2\Psi. \quad (20)$$

This gives the coarse-grained dynamics.

### Derivation 2: Small $k$ expansion of Tkachenko's solution

In this section we follow Tkachenko's work [13, 14] and consider an infinite lattice,  $\Lambda$ , of  $2\pi$  strength vortices ( $\Gamma_{mn} = 2\pi$ ) at sites  $z_{mn}^0 = 2me_1 + 2ne_2$ , with the half-periods  $e_1, e_2 \in \mathbb{C}$ , and  $m, n \in \mathbb{Z}$ . Extending the finite

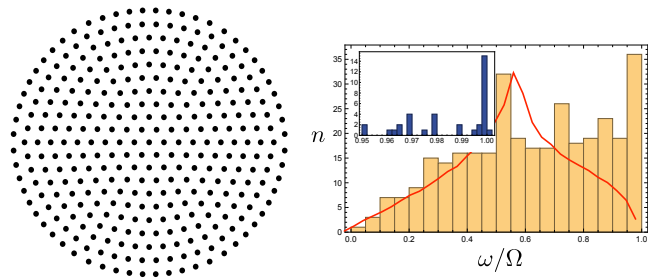


Figure 2. Left: equilibrium configuration for  $s = 10$ ,  $N = 331$  vortices. For  $\omega = 1$ , radius is equal to 17.44. The vortices form a distorted hexagonal lattice, note the outer circle is rotated by half a lattice consistent with Campbell and Ziff [10, 11]. Right: numerically calculated density of states for  $N = 331$  (totalling 331). Red line shows the continuum limit, note the absence of a frequencies near  $\omega/\Omega = 1$  in this case. Inset: cluster of frequencies close to  $\omega/\Omega = 1$ , corresponding to anti-holomorphic modes.

vortex expression to the infinite lattice leads to divergent sums for the velocity field. However, the Weierstrass  $\zeta$  function has the requisite poles, so the velocity field associated to the lattice must be given by

$$\overline{v(z)} = \frac{1}{i}(\zeta(z; \Lambda) + f(z)), \quad (21)$$

where  $f(z)$  is an entire function. As shown by Tkachenko, if  $\Lambda$  is a triangular lattice, then setting  $f(z) = 0$  and using properties of the Weierstrass  $\zeta$  function gives a velocity field describing a steady rigid rotation of the lattice, with angular frequency  $\Omega = \pi/4 \text{Im}(\bar{e}_1 e_2)$ .

Near  $z = 0$  the Weierstrass zeta function satisfies

$$\zeta(z) = \frac{1}{z} - \sum_{k=1}^{\infty} \mathcal{G}_{2k+2}(\Lambda) z^{2k+1}, \quad (22)$$

where  $\mathcal{G}_{2k+2}(\Lambda)$  is the Eisenstein series of weight  $2k+2$ ,  $\mathcal{G}_4 = g_2/60$  and  $\mathcal{G}_6 = g_3/140$ . For the triangular lattice  $g_2 = 0$ . (22) implies that the  $(0, 0)$  vortex is stationary if  $f(0) = 0$ . The  $\zeta$  function satisfies

$$\zeta(z + z_{mn}) = \zeta(z) + 2m\zeta(e_1) + 2n\zeta(e_2), \quad (23)$$

$$e_2\zeta(e_1) - e_1\zeta(e_2) = i\frac{\pi}{2}. \quad (24)$$

From this, the velocity field at each lattice point is found to be

$$\overline{v_{mn}} = \frac{1}{i}(2m\zeta(e_1) + 2n\zeta(e_2) + f(z_{mn}^0)). \quad (25)$$

We choose  $f(z) = \alpha z$ ,  $\alpha \in \mathbb{C}$ , linear so that

$$\zeta(e_1) + \alpha e_1 = \Omega \bar{e}_1, \quad (26)$$

where  $\Omega = \pi/4 \text{Im}(\bar{e}_1 e_2)$ , from this it follows that

$$\zeta(e_2) + \alpha e_2 = \Omega \bar{e}_2, \quad (27)$$

and we find the velocity at each vortex is given by

$$v_{mn} = i\Omega(2me_1 + 2ne_2), \quad (28)$$

describing a rigid rotation with angular velocity  $\Omega$ . For the triangular lattice, the focus here,  $\alpha = 0$ , which we take henceforth. Concretely we set  $e_1 \in \mathbb{R}$ ,  $e_2 = e^{i2\pi/6}e_1$ . Suppose now we perturb the lattice, writing  $z_{mn} = z_{mn}^0 + \epsilon_{mn}$ , we suppose the perturbations are in  $\ell^2(\mathbb{Z}^2)$ , so that

$$\sum_{\Lambda} |\epsilon_{mn}|^2 < \infty. \quad (29)$$

Then the velocity field can be written as

$$\bar{v}(z) = \frac{1}{i} \left( \zeta(z) + \sum_{m,n} \frac{1}{z - z_{mn}^0 - \epsilon_{mn}} - \frac{1}{z - z_{mn}^0} \right), \quad (30)$$

To first order in  $\{\epsilon_{mn}\}$ , the velocity of vortex  $(m, n)$  may then be written as

$$\begin{aligned} \overline{v(z_{mn})} &= -i\Omega(2m\bar{e}_1 + 2n\bar{e}_2) \\ &- i \sum_{(m',n') \neq (m,n)} \frac{\epsilon_{m'n'}}{(z_{m'n'}^0 - z_{mn}^0)^2} + O(\epsilon^2) \end{aligned} \quad (31)$$

This yields the equation of motion (at  $t = 0$ )

$$\frac{d}{dt} \epsilon_{mn} = i \sum_{(m',n') \neq (m,n)} \frac{\bar{\epsilon}_{m'n'}}{(\bar{z}_{m'n'}^0 - \bar{z}_{mn}^0)^2} \quad (32)$$

To obtain the full equations of motion we pass to the rotating frame  $\epsilon_{mn} = e^{i\Omega t} \psi_{mn}$ , finding

$$\frac{d}{dt} \psi_{mn} = -i\Omega \psi_{mn} + i \sum_{(m',n') \neq (m,n)} \frac{\bar{\psi}_{m'n'}}{(\bar{z}_{m'n'}^0 - \bar{z}_{mn}^0)^2}. \quad (33)$$

Now let  $b_1, b_2 \in \mathbb{C}$  be reciprocal lattice vectors satisfying  $\text{Re}(2e_i \bar{b}_j) = 2\pi \delta_{ij}$  and  $BZ \subset \mathbb{C}$  the Brillouin zone. The area of the Brillouin zone is  $(2\pi)^2 \Omega / \pi$ . Then, writing  $k = k_1 b_1 + k_2 b_2 \in BZ$ , we may expand  $\psi_{mn}$  in plane waves as

$$\psi_{mn} = \frac{\pi}{\Omega(2\pi)^2} \int_{BZ} \psi(k) e^{i2\pi(k_1 m + k_2 n)} dA_k \quad (34)$$

with

$$\psi(k) = \sum_{m,n} e^{-i2\pi(k_1 m + k_2 n)} \psi_{mn}. \quad (35)$$

$\psi(k)$  is then found to satisfy the equation

$$\dot{\bar{\psi}}(k) = i\Omega \bar{\psi}(k) \quad (36)$$

$$-i \sum_{(m,n)} \sum_{(m',n') \neq (m,n)} \frac{\psi_{m'n'} e^{-i2\pi(k_1 m + k_2 n)}}{4((m' - m)e_1 + (n' - n)e_2)^2} \quad (37)$$

We can rewrite this as

$$\dot{\bar{\psi}}(k) = i\Omega \bar{\psi}(k) - i \sum_{(m',n')} \beta(k) \psi_{m'n'} e^{-i2\pi(k_1 m' + k_2 n')}, \quad (38)$$

where  $\beta$  is given as

$$\beta = \sum_{(m,n) \neq (m',n')} \frac{e^{-i2\pi(k_1(m-m') + k_2(n-n'))}}{4((m' - m)e_1 + (n' - n)e_2)^2} \quad (39)$$

$$= \sum_{(m,n) \neq (0,0)} \frac{e^{2\pi i(k_1 m + k_2 n)}}{4(m e_1 + n e_2)^2}. \quad (40)$$

$\beta$  is a function of  $k = k_1 b_1 + k_2 b_2$ , where  $b_1 = -2\Omega i e_2$ ,  $b_2 = 2\Omega i e_1 \in \mathbb{C}$  are reciprocal lattice vectors (recall the lattice vectors are  $2e_1$  and  $2e_2$ ). In fact, as shown by Tkachenko [14],  $\beta$  is more readily written in terms of  $\kappa = 2(k_1 \bar{e}_2 - k_2 \bar{e}_1) = -i\bar{k}/2\Omega$ , evaluating gives

$$\beta(\kappa) = \frac{1}{2} (\wp(\kappa) - \zeta(\kappa)^2) + \Omega \bar{\kappa} \zeta(\kappa) - \frac{1}{2} \Omega^2 \bar{\kappa}^2, \quad (41)$$

where  $\wp$  is the Weierstrass p-function. This then yields the evolution equation for  $\bar{\psi}(k)$

$$\frac{d}{dt} \bar{\psi}(k) = -i\Omega \bar{\psi}(k) + i\beta \bar{\psi}(k) = H \bar{\psi}(k). \quad (42)$$

Considering  $H$  as a real  $2 \times 2$  matrix, let  $\pm i\omega(k) = \pm i\sqrt{\Omega^2 - |\beta(k)|^2}$  denote the eigenvalues of  $H$ . For the triangular lattice,  $\omega$  is real and non-zero except at  $k = 0$ , as shown by Tkachenko, reflecting the stability of the lattice. Expanding  $\beta(k)$  close to zero gives

$$\beta(k) = -\Omega \frac{k^2}{|k|^2} \left( 1 - \frac{|k|^2}{8\Omega} \right) + \frac{\mathcal{G}_6}{64\Omega^4} \left( 14 - \frac{|k|^2}{\Omega} \right) \bar{k}^4 + O(k^8). \quad (43)$$

Near  $k = 0$  we have  $|\omega| \approx \sqrt{\Omega}|k|/2$ , the Tkachenko frequency. Up to order  $|k|^2$  the dispersion relation is isotropic, coarse-graining at this level should therefore yield an appropriate linearized long-wavelength theory.

Now consider the long-wavelength dynamics of  $\psi(k)$  for  $|k|^2 \ll \Omega$ ,

$$i\partial_t \psi(k) = \Omega \psi(k) + \Omega \frac{k^2}{|k|^2} \left( 1 - \frac{|k|^2}{8\Omega} \right) \bar{\psi}(k). \quad (44)$$

we rewrite as

$$i\partial_t \bar{\psi}(k) = -\Omega \bar{\psi}(k) - \Omega \frac{\bar{k}^2}{|k|^2} \psi(k) + \frac{\bar{k}^2}{8} \psi(k). \quad (45)$$

Returning to real space we define

$$\Psi(z) = \int_{\mathbb{C}} \psi(k) e^{i(k_x x + k_y y)} dA_k \quad (46)$$

where  $z = x + iy \in \mathbb{C}$ , which yields

$$i\partial_t \bar{\Psi}(z) = -\Omega \bar{\Psi} + 4\pi\Omega \int \frac{\Psi(w)}{(z-w)^2} dA_w - \frac{1}{2} \frac{\partial^2}{\partial z^2} \Psi. \quad (47)$$

where the integral is over the entire domain. This reproduces (20) except for the factor of  $\Psi(z)$  in the non-local term. This factor gives zero in a disk domain (our focus), so the two theories agree. This arises, as Tkachenko notes [14], because the Weierstrass  $\zeta$  function is not simply the sum of flow fields due to each vortex in the lattice.

### ANTI-HOLOMORPHIC MODES

We now suppose the vortex lattice forms a disc  $D$  of radius  $R$ . In this case we have

$$\Psi(z) \int_D \frac{1}{(z-w)^2} dA_w = 0 \quad (48)$$

and we find the system, using either theory,

$$i\partial_t \bar{\Psi} = -\Omega \bar{\Psi} + 4\pi\Omega \int_D \frac{\Psi(w)}{(z-w)^2} dA_w - \frac{1}{2} \frac{\partial^2}{\partial z^2} \Psi. \quad (49)$$

Numerical work [29] suggests the existence of modes that counter-rotate with the lattice at frequency  $\Omega$ . We further

suppose that the trajectories traced out by the perturbed vortices are circular, *i.e.*  $|\Psi|$  is constant in time. Such modes are therefore solutions of the equation

$$\frac{1}{\pi} \int_D \frac{\Psi(w)}{(z-w)^2} dA_w - \frac{1}{C} \frac{\partial^2}{\partial z^2} \Psi = 0. \quad (50)$$

A first integral gives

$$\frac{\partial}{\partial z} \left( \frac{1}{\pi} \int_D \frac{\Psi(w)}{w-z} dA_w - \frac{1}{C} \frac{\partial}{\partial z} \Psi \right) = 0, \quad (51)$$

where  $C = 8\Omega\pi^2$ . The Cauchy-Pompeiu formula yields

$$\frac{\partial}{\partial z} \left( -\eta(z) + \frac{1}{2\pi i} \int_{\partial D} \frac{\eta(w)}{w-z} dw - \frac{\partial}{\partial z} \frac{\partial}{\partial \bar{z}} \eta \right) = 0, \quad (52)$$

where  $\Psi(z) = \frac{\partial \eta}{\partial \bar{z}}$ . Now we suppose an expansion

$$\eta = \bar{z} \sum_{a,b=0}^{\infty} c_{ab} z^a \bar{z}^b. \quad (53)$$

We then obtain

$$\sum_{a,b} \left( -ac_{ab} z^{a-1} \bar{z}^{b+1} - \frac{1}{C} a(a-1)(b+1) c_{ab} z^{a-2} \bar{z}^b + R^{2(b+1)} \begin{cases} 0 & a-b \leq 0 \\ (a-b-1) c_{ab} z^{a-b-2} & a-b > 0 \end{cases} \right) = 0. \quad (54)$$

To solve this system of equations we identify three distinct regimes. Firstly, any antiholomorphic function  $\eta(\bar{z})$  is clearly a solution. Gathering powers of  $z$  and (non-zero)  $\bar{z}$  yields the equation

$$c_{a+1,b+1} = -C \frac{c_{ab}}{(a+1)(b+2)}, \quad a \neq 0. \quad (55)$$

To proceed we look at all terms in (53) with a constant value of  $s = b - a$ , with  $a \neq 0$ . We first consider  $s \geq 0$ . Gathering terms with non-zero powers of  $\bar{z}$  we use (55) and find

$$c_{i,i+s} = c_{1,1+s} \frac{(-C)^{i-1} (2+s)!}{i!(1+i+s)!}. \quad (56)$$

The resulting series can be summed to yield

$$-c_{0,s} (2+s)_0 F_1(2+s; -C|z|^2) = f_s, \quad (57)$$

where  ${}_0F_1$  is a generalized hypergeometric function. We

now consider  $s < 0$ . Once again we use (55) and find

$$c_{i-s,i} = c_{-s,0} \frac{(-C)^i (-s)!}{(i+1)!(i-s)!}. \quad (58)$$

Gathering terms with no powers of  $\bar{z}$  yields the additional condition for  $s < 0$

$$-(1+s) \left( \frac{s}{C} c_{-s,0} + \sum_{b=0} R^{2(b+1)} c_{-s+b,b} \right) = 0, \quad (59)$$

which is incompatible with (58) for  $s \neq -1$ . We therefore find a single additional solution, summing coefficients in (58) for  $s = -1$  gives

$$\frac{1 - {}_0F_1(1; -C|z|^2)}{C|z|^2} = f_{-1}. \quad (60)$$

We therefore find a general solution of the form

$$\Psi = \gamma f_{-1} z + \sum_{s=0}^{\infty} (\alpha_s + \beta_s f_s) \bar{z}^s, \quad (61)$$

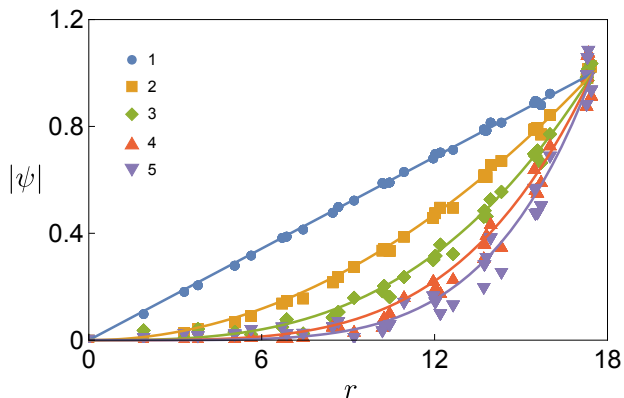


Figure 3.  $|\psi|$  as a function of radial distance,  $r$ , for the first five anti-holomorphic modes. Dots are numerical data scaled so that the average value on the outer circle ( $r \approx 17$ ) is 1, solid lines show  $r^n$ , scaled to be equal to one at the outer circle. No other fitting is performed.

where  $\alpha_s, \beta_s, \gamma \in \mathbb{C}$  are constants. In our coarse-grained theory we expect  $|z|$  to be large compared to the lattice lengthscale,  $1/\sqrt{C}$ . In this limit,  $f_{-1} \sim 1/(C|z|^2)$  and  $f_s$ ,  $s \geq 0$ , tends to a constant (which we absorb into  $\alpha_s$ ). We therefore find

$$\Psi \approx \sum_{s=0}^{\infty} \alpha_s \bar{z}^s, \quad (62)$$

an arbitrary anti-holomorphic function. We note that these solutions are the only ones that survive if we drop the  $\partial_z^2 \psi$  term in the coarse-grained theory.

## NUMERICS

For a finite vortex lattice, we define a mode of the full (non-coarse-grained) linear system with  $\Psi(z) \approx \bar{z}^n$  as the  $n^{\text{th}}$  anti-holomorphic mode of the vortex lattice. The  $n^{\text{th}}$  mode at any given point in time gives rise to an emergent deformation structure of  $n + 1$  radial peaks and troughs around the edge of the system, as illustrated in Figure 1. We can expect to observe these modes only while  $n \ll \Omega R^2$ , where  $R$  is the radius of the entire lattice. Additionally, we expect that for eigenmodes of finite lattice, the anti-holomorphic functions appear only approximately, with the degeneracy broken. In general then we expect that large but finite steadily rotating vortex lattices should have normal modes  $\Psi(z)$  with the following properties (in the frame corotating with the lattice):

1.  $\Psi(z)$  is approximately anti-holomorphic,

2. The normal mode counter rotates with angular frequency close to  $\Omega$ ,
3. The paths traced out by the perturbed vortices are close to circular.

In this section we compare the prediction of the theory to numerical simulations. We consider a set of  $N$  vortices in the plane all with equal circulations,  $\Gamma_i = 2\pi$ . We first numerically minimise the rotating-frame Hamiltonian to find an equilibrium configuration for  $N$  vortices. We take  $N$  to be the number  $C_s$ ,  $s \geq 0$ ,

$$C_s = 1 + 6 \sum_{i=0}^s s = 1 + 3s(1 + s), \quad (63)$$

which is the number of points a lattice distance at most  $s$  from the origin in a triangular lattice. The vortices are initialized at the origin and the points  $z_{ab} = ae^{i2\pi b/6a}$ , where  $a$  runs from 1 through  $s$ ,  $b$  from 0 to  $6a - 1$ . The energy (7) (with  $\Omega = 1$ , varying  $\Omega$  simply acts as a scaling for the lattice) is then minimized. This is done using the L-BFGS algorithm in Python (`scipy.optimize`). An example configuration is shown for  $s = 10$  in Fig. 2, the minimum is a distorted triangular lattice. We note here that Campbell and Ziff [10, 11] find the global minimum energy for configurations of  $C_s$  vortices having the outer circle rotated by half a lattice constant, a result we reproduce. The results we show are for  $s = 10$  ( $N = 331$ ), chosen to be sufficiently large to observe the anti-holomorphic modes and sufficiently small to be easily accessible to precise computation.

Once the equilibrium configuration is found, the eigenvalues and eigenvectors of the linearized theory are computed. As expected from the theory, we find broadly two classes of modes, bulk modes with frequency  $\omega < \Omega$  and a collection of modes with  $\omega \approx \Omega$ , the candidate anti-holomorphic modes. The density of states is shown in Fig. 2. We note here that the density of states arising from Tkachenko's solution does not produce this excess of modes near  $\Omega$ , reflecting the fact that the anti-holomorphic modes do not exist in the infinite system.

In the coarse-grained theory, anti-holomorphic functions are a degenerate eigenspace with frequency  $\Omega$ . In the real system this degeneracy is broken by microscopic details, and we find a collection of modes with frequencies just below  $\Omega$ . For example, the second eigenmode is found to have frequency  $0.9999998\Omega$ . The non-constant eigenmodes are observed to be linear combinations of different anti-holomorphic modes, with  $\Psi$  constant appearing as an exact solution with frequency  $\Omega$  for all stable vortex crystals. For example, the  $n = 1$  anti-holomorphic mode is found to be a linear combination of the second and third eigenmodes of the lattice system. As linear combinations of powers of  $\bar{z}$ ,

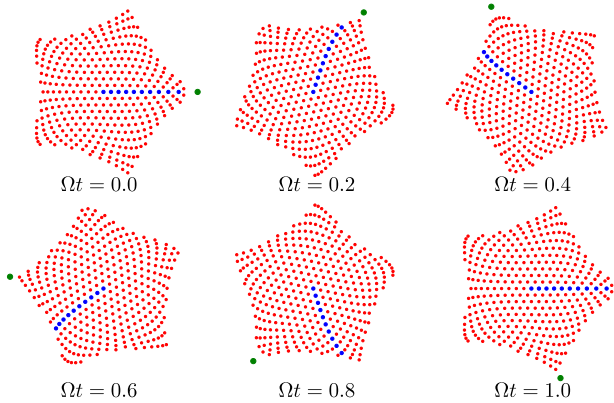


Figure 4. The  $n = 4$  mode. A reference set of vorticities are highlighted in blue, and orbit the center with angular frequency  $\Omega$ . A reference deformation peak is indicated by the green dot, and orbits the center with angular velocity  $\frac{n}{n+1}\Omega$ .

the eigenmodes appear as power-law confined chiral edge modes of the vortex lattices.

To extract the ‘pure’ anti-holomorphic modes  $\sim \bar{z}^n$ , we consider linear combinations of the  $M$  numerically obtained modes with frequencies closest to  $\Omega$ .  $M$  was chosen, empirically, to be 16. We then take the ‘outer circle’ of  $s$  vorticities (see (63)) and find the complex linear combination of the  $M$  modes that gives the best least-squares fit to  $\bar{z}^n$  on the outer circle. The resulting modes are shown in Fig. 1 for  $1 \leq n \leq 6$ . To assess the accuracy we plot the magnitude  $|\psi|$  as a function of radius  $r$ , which should scale as  $r^n$ . This is shown in Fig. 3, for  $1 \leq n \leq 5$  we find excellent agreement, for higher  $n$  the correspondence begins to break down, as we would expect. It is important to note that the pure  $\bar{z}^n$  modes are only approximate eigenmodes of the system, becoming exact as the lattice size goes to infinity.

How do these modes appear in the lab frame? In the rotating frame, each vortex rotates about a lattice point with angular frequency  $-\Omega$ . However, in the lab frame the whole system rotates with angular frequency  $\Omega$ , as such each vortex is displaced from the lattice by a time independent vector. In particular, from this we can find that the maxima of radius appear at  $\theta$  obeying

$$\theta = \frac{n}{n+1}\Omega t + \frac{2\pi}{n+1}p, \quad (64)$$

where  $p \in 1, 2, \dots, n$ . We then see the second term defines the  $n+1$  peaks, and the first term tells us that this emergent structure rotates with frequency

$$\frac{n}{n+1}\Omega, \quad (65)$$

as depicted in Figure 4. This difference in frequencies is

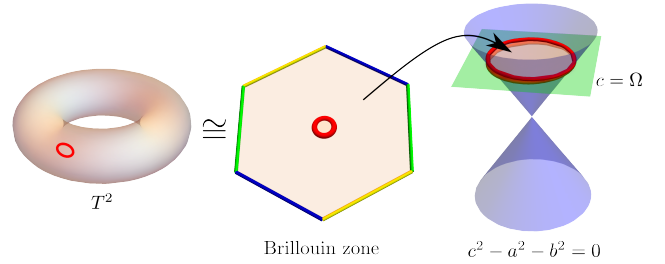


Figure 5. Left/Middle: The Brillouin zone with a puncture at  $k = 0$ . A loop (red) around the puncture, when shrunk to the origin, is mapped to a loop winding twice around the surface of the cone. The rest of the Brillouin zone is not defective and so does not map to the surface of the cone. Right: The set of defective Hamiltonians form a cone (blue), with the frequency  $\Omega$  dictating the height (green).

analogous to the difference in frequencies associated to solar days and sidereal days as a planet orbits a star; as the lattice point orbits the center, the direction of the perturbation required to create a deformation peak is also shifted.

## BULK-BOUNDARY CORRESPONDENCE

The non-constant anti-holomorphic modes we describe cannot appear in an infinite system, by Liouville’s theorem they are not bounded, and so cannot be realized as perturbations of a lattice in any physically meaningful sense. However, as demonstrated by the numerical results, in a large but finite system they appear, albeit approximately. If one considers the non-constant anti-holomorphic modes as (power-law confined) edge waves, this can be considered as a kind of bulk-boundary correspondence. In fact, their existence can be ascribed to the  $k = 0$  singularity in Tkachenko’s solution. The Hamiltonian nature of the original vortex system ensures that, as a real linear operator on  $\tilde{\psi}(k)$ ,  $H(k) \in \mathfrak{sl}(2, \mathbb{R})$ , the Lie algebra of traceless  $2 \times 2$  matrices.  $H(k)$  has a singularity at  $k = 0$ , the bulk spectrum of the vortex lattice therefore defines a map from the punctured Brillouin zone into  $\mathfrak{sl}(2, \mathbb{R})$ , as

$$H(k) : BZ \setminus \{0\} \rightarrow \mathfrak{sl}(2, \mathbb{R}). \quad (66)$$

We may write a general element of  $\mathfrak{sl}(2, \mathbb{R})$  as

$$X = \begin{pmatrix} a & b+c \\ b-c & -a \end{pmatrix}, \quad (67)$$

The set of defective Hamiltonians with this symmetry can be identified with the cone  $c^2 - a^2 - b^2 = 0$ , null vectors in Minkowski space  $\mathbb{M}^{2,1}$ . Excluding the origin in  $\mathfrak{sl}(2, \mathbb{R})$  gives the set of defective Hamiltonians the homotopy type

of two disjoint circles. We now consider the explicit form of the spectrum for the vortex lattice, near  $k = 0$  we may write

$$H(k) = -\Omega \begin{bmatrix} \sin 2\theta_k & \cos 2\theta_k - 1 \\ \cos 2\theta_k + 1 & -\sin 2\theta_k \end{bmatrix} \quad (68)$$

$$+ \frac{|k|^2}{8} \begin{bmatrix} \sin 2\theta_k & \cos 2\theta_k \\ \cos 2\theta_k & -\sin 2\theta_k \end{bmatrix} + \mathcal{G}_3 O((|k|/\Omega)^4)$$

The overall rotation of the lattice forces  $c = \Omega$  in (67). Coupled with Tkachenko's dispersion relation  $|\omega| \approx \sqrt{\Omega}|k|/2$ , we see that as a small loop around  $k = 0$  is shrunk to the origin in the Brillouin zone, the image under the map  $H(k)$  is a loop winding around the cone of defective matrices, with winding number 2. The local structure of this singularity is sufficient to reproduce the anti-holomorphic modes.

### ACKNOWLEDGEMENTS

We thank T. Gavrilchenko, J.M.F. Gunn, J.H. Hannay, Y. Hu, and R.D. Kamien for helpful discussions. This work was supported by the EPSRC through grant EP/T517872/1.

---

\* t.machon@bristol.ac.uk

- [1] H. Helmholtz, About integrals of hydrodynamic equations related with vortical motions, *J. für die reine Angewandte Mathematik* **55**, 25 (1858).
- [2] E. Yarmchuk, M. Gordon, and R. Packard, Observation of stationary vortex arrays in rotating superfluid helium, *Phys. Rev. Lett.* **43**, 214 (1979).
- [3] J. R. Abo-Shaeer, C. Raman, J. M. Vogels, and W. Ketterle, Observation of vortex lattices in bose-einstein condensates, *Science* **292**, 476 (2001).
- [4] T. Mitchell, C. Driscoll, and K. Fine, Experiments on stability of equilibria of two vortices in a cylindrical trap, *Phys. Rev. Lett.* **71**, 1371 (1993).
- [5] D. Durkin and J. Fajans, Experiments on two-dimensional vortex patterns, *Phys. Fluids* **12**, 289 (2000).
- [6] K. Fine, A. Cass, W. Flynn, and C. Driscoll, Relaxation of 2d turbulence to vortex crystals, *Phys. Rev. Lett.* **75**, 3277 (1995).
- [7] H. Aref, Point vortex dynamics: a classical mathematics playground, *J. Math. Phys.* **48**, 065401 (2007).
- [8] P. K. Newton, *The N-vortex problem: analytical techniques*, Vol. 145 (Springer Science & Business Media, 2013).
- [9] H. Aref, P. K. Newton, M. A. Stremler, T. Tokieda, and D. L. Vainchtein, Vortex crystals, *Advances in applied Mechanics* **39**, 2 (2003).
- [10] L. Campbell and R. Ziff, *Catalog of two-dimensional vortex patterns*, Tech. Rep. (Los Alamos Scientific Lab., NM (USA), 1978).
- [11] L. J. Campbell and R. M. Ziff, Vortex patterns and energies in a rotating superfluid, *Phys. Rev. B* **20**, 1886 (1979).
- [12] Y. Chen, T. Kolokolnikov, and D. Zhirov, Collective behaviour of large number of vortices in the plane, *Proc. R. Soc. A* **469**, 20130085 (2013).
- [13] V. Tkachenko, On vortex lattices, *Sov. Phys. JETP* **22**, 1282 (1966).
- [14] V. Tkachenko, Stability of vortex lattices, *Sov. Phys. JETP* **23**, 1049 (1966).
- [15] E. B. Sonin, Tkachenko waves, *JETP Letters* **98**, 758 (2014).
- [16] V. Tkachenko, Elasticity of vortex lattices, *Sov. Phys. JETP* **29**, 945 (1969).
- [17] E. Sonin, Vortex oscillations and hydrodynamics of rotating superfluids, *Rev. Mod. Phys.* **59**, 87 (1987).
- [18] I. Coddington, P. Engels, V. Schweikhard, and E. A. Cornell, Observation of tkachenko oscillations in rapidly rotating bose-einstein condensates, *Physical review letters* **91**, 100402 (2003).
- [19] J. Noronha and A. Sedrakian, Tkachenko modes as sources of quasiperiodic pulsar spin variations, *Physical Review D* **77**, 023008 (2008).
- [20] M. Ruderman, Long period oscillations in rotating neutron stars, *Nature* **225**, 619 (1970).
- [21] B. Haskell, Tkachenko modes in rotating neutron stars: the effect of compressibility and implications for pulsar timing noise, *Physical Review D* **83**, 043006 (2011).
- [22] D. Leykam, K. Y. Bliokh, C. Huang, Y. D. Chong, and F. Nori, Edge modes, degeneracies, and topological numbers in non-hermitian systems, *Phys. Rev. Lett.* **118**, 040401 (2017).
- [23] Z. Gong, Y. Ashida, K. Kawabata, K. Takasan, S. Higashikawa, and M. Ueda, Topological phases of non-hermitian systems, *Phys. Rev. X* **8**, 031079 (2018).
- [24] K. Sone, Y. Ashida, and T. Sagawa, Exceptional non-hermitian topological edge mode and its application to active matter, *Nat. Commun.* **11**, 1 (2020).
- [25] P. Wiegmann, Hydrodynamics of euler incompressible fluid and the fractional quantum hall effect, *Phys. Rev. B* **88**, 241305 (2013).
- [26] P. Wiegmann and A. G. Abanov, Anomalous hydrodynamics of two-dimensional vortex fluids, *Phys. Rev. Lett.* **113**, 034501 (2014).
- [27] G. Volovik and V. Dotsenko, Hydrodynamics of defects in condensed media, using as examples vortices in rotating he ii and disclinations in a planar magnet, *Soviet Phys. JETP* **78**, 132 (1980).
- [28] G. Baym and E. Chandler, The hydrodynamics of rotating superfluids. i. zero-temperature, nondissipative theory, *J. Low Temp. Phys.* **50**, 57 (1983).
- [29] L. Campbell, Transverse normal modes of finite vortex arrays, *Phys. Rev. A* **24**, 514 (1981).
- [30] L. Campbell, Transverse vortex oscillations in finite patterns, *Physica B + C* **108**, 1375 (1981).
- [31] L. Campbell and Y. K. Krasnov, Edge waves of a vortex continuum, *Phys. Lett. A* **84**, 75 (1981).
- [32] E. B. Sonin, *Dynamics of quantised vortices in superfluids* (Cambridge University Press, 2016).
- [33] M. Cazalilla, Surface modes of ultracold atomic clouds with a very large number of vortices, *Phys. Rev. A* **67**, 063613 (2003).



- [34] A. Bogatskiy and P. Wiegmann, Edge wave and boundary layer of vortex matter, *Phys. Rev. Lett.* **122**, 214505 (2019).
- [35] V. P. Patil and J. Dunkel, Chiral edge modes in helmholtz-onsager vortex systems, *Phys. Rev. Fluids* **6**, 064702 (2021).
- [36] T. Lundgren and Y. Pointin, Statistical mechanics of two-dimensional vortices, *J. Stat. Phys.* **17**, 323 (1977).
- [37] R. M. Menezes and C. C. de Souza Silva, Conformal vortex crystals, *Sci. Rep.* **7**, 1 (2017).
- [38] E. Sonin, Vortex-lattice vibrations in a rotating helium ii, *J. Exp. Theor. Phys.* **43**, 1027 (1976).
- [39] E. Sonin, Continuum theory of tkachenko modes in rotating bose-einstein condensate, *Phys. Rev. A* **71**, 011603 (2005).
- [40] G. Baym, Tkachenko modes of vortex lattices in rapidly rotating bose-einstein condensates, *Phys. Rev. Lett.* **91**, 110402 (2003).
- [41] J. Anglin and M. Crescimanno, Inhomogeneous vortex matter, arXiv preprint cond-mat/0210063 (2002).
- [42] S. Moroz, C. Hoyos, C. Benzoni, and D. T. Son, Effective field theory of a vortex lattice in a bosonic superfluid, *SciPost Phys.* **5** (2018).